Simulations of atomic structure, dynamics, and self-diffusion in liquid Au

Alexander Bogicevic, Lars B. Hansen, and Bengt I. Lundqvist

Department of Applied Physics, Chalmers University of Technology and Göteborg University, S-412 96 Göteborg, Sweden

Static and dynamic properties of liquid Au are studied with molecular-dynamics and Monte Carlo simulations, using a many-body potential based on the effective-medium theory. In order to address the outstanding question about the temperature dependence of the self-diffusion coefficient (linear, exponential, and other dependencies have been proposed in the literature), simulations are performed in a dense temperature mesh up to the boiling point (3080 K). The liquid structure at various temperatures is described in terms of the pair distribution function, which is compared with x-ray data. Computed thermodynamic properties are in good agreement with experiment. Dynamic properties are represented by the velocity correlation function and self-diffusion coefficients of high accuracy. The temperature dependence of the diffusivity is qualitatively compared with several theoretical model predictions. A proportionality of the diffusion coefficient to the square of the temperature is found, in agreement with recent microgravity experiments on other nonsimple liquids. An analysis is made of atomic trajectories and the velocity correlation function at various temperatures, to provide physical arguments for and against different diffusion models in liquids. One of the results of this study is that it opposes diffusion processes with a single nonzero activation energy of, e.g., Arrhenius type. A discussion on this topic is included. [S1063-651X(97)04305-5]

PACS number(s): 66.10.−x, 61.20.Ja

I. INTRODUCTION

Liquids are less understood than solids and gases [1,2]. The major reason for this is the fact that, unlike for solids and gases, there exists no idealized model for liquids. Yet, the liquid state is one of the fundamental states of matter, a fact that by itself calls for an understanding of, e.g., structural, dynamical, and transport properties. In addition, there are important applications.

An understanding of the diffusion processes in liquid metals and metal alloys is of great importance for, e.g., the metallurgical industry. Many metallic materials are manufactured after careful refining in the molten state, where diffusion coefficients are essential ingredients in calculating chemical rate constants. The diffusion of atoms through a supersaturated alloy is a fundamental step in the vapor-liquid-solid (VLS) mechanism of single-crystal whisker growth. In close connection to this, the distribution of solute atoms during solidification also crucially depends on their diffusive motion. Towards this background, it is surprising that it is still today very hard to find experimental data on diffusion coefficients for most systems, and that the existing theoretical and empirical descriptions of liquids have met limited success.

The best covered liquids are undoubtedly the condensed group-VIII rare-gas atoms, together with the group-I alkali-metal atoms. The equilibrium properties of these simple liquids have been well understood for decades. For dynamics of liquids there has also been a substantial amount of progress [1]. Important contributions have been made to the general theory of time-correlation functions [3], at least for liquids under ordinary thermodynamic conditions, even though the area is not as settled as the one for the corresponding equilibrium properties.

For simple liquids, a considerable effort has been put into computer simulations, attempting to bridge the gap between theory and experiment. The soul of any simulation lies in the potential used in describing the interaction of its constituents. Therefore, in order to theoretically examine a liquid in a meaningful way, it is essential to have some form of physically sound model potential. One of the simplest descriptions of a liquid is given by the so-called hard-sphere model, which is of purely repulsive nature [1]. This model has only one adjustable parameter, the hard-sphere diameter. By this simplification of the atomic interactions, it is possible to analytically calculate various properties of the hard-sphere ''liquid.''

One variety of the hard-sphere model is accomplished by adding a square-well attractive part extending some distance away from the shell of the sphere [1]. Another common, and smoother, interatomic potential for simple liquids is the so-called Lennard-Jones 6-12 potential, which has two parameters, the collision diameter and the potential depth. Models of this kind rely on computer simulations for the calculation of various system properties.

All of these pair-potential models can fairly well reproduce the experimentally obtained structures of at least some simple liquids, typically expressed in the form of distribution functions [4,5]. By allowing the hard-sphere diameters to be temperature dependent, the diffusion behavior at various temperatures can sometimes be well accounted for [6]. These are remarkable results. They owe their fact to the predominant repulsive short-range behavior stemming from the Pauli principle, preventing overlap of the outer electron shells. All candidate interaction potentials must incorporate this sharp short-range repulsive feature; this is also the case for the models mentioned above. The attractive forces, acting at long range, vary much more smoothly. While minimally influencing the structure, these forces provide an attractive background that gives rise to the cohesive energy required to stabilize the liquid. The analytical theory proposed by Weeks, Chandler, and Andersen [7] in the 1970s, in particu-

lar, makes it clear precisely how the sharply repulsive part of a model interatomic potential (Lennard-Jones) determines liquid structure, and how thermodynamics is explained by little more than a mean-field correction arising from the remainder of the potential.

Ordinary pair potentials, the most common one being the Lennard-Jones potential mentioned above, have been widely used to describe metallic liquids. Even for simple liquids, however, experiments have shown the effective pair potential to have a form different from the Lennard-Jones one. Of course, progress has been made, owing to the relatively simple electron structure of the group-VIII and -I atoms. In fact, most of what we know about (simple) liquids stems from the pioneering work on hard-sphere and Lennard-Jones liquids performed during the last three decades.

These kinds of potentials omit a crucial piece of the physics of metallic bonding, however, and attempts to treat other than simple metals have not met the same success. For instance, all purely pairwise-potential models produce the Cauchy relation between the elastic constants, $C_{12}/C_{44}=1$, which does not apply for real metals, where this ratio for, e.g., Au, is 3.7 [8]. The nonpairwise potential used in this paper improves on this considerably, see below. Also, the pairwise models fail to describe surface properties, such as surface relaxation [9], adequately. Defects are also poorly described [10]. For instance, the vacancy formation energy is strongly overestimated. Other problems with pair potentials include overestimated melting temperatures and entropy changes on melting [10]. Most computer simulations of liquids utilize effective pair potentials that are optimized by some kind of a fitting procedure in order to describe the system well at a certain temperature, pressure, or density. Such an approach requires different potentials at, e.g., different temperatures. Thus such potentials have limited value for assessing the temperature dependence of, e.g., the diffusion coefficient.

The end of the 1980s saw the birth of improved many-body-interaction potentials, such as the embedded-atom method (EAM) [11], the glue model (GM) [12], and the effective-medium theory (EMT) [13]. These theories have proven their quality in a variety of fields within the solid state: segregation, alloying, melting, point defects, dislocations, and surface structures are just a few examples [8,14,15]. The combination of many-body calculational schemes that scale linearly with the number of atoms rather than cubically, and improvements in raw computer power provide a basis that should put computer simulations of liquids into a renaissance.

The main purpose of this work is to simulate the atomic self-diffusion in pure liquid gold over the entire liquid temperature range using a many-body EMT potential. Gold is chosen for several reasons. It is a noble metal, i.e., nonsimple. Furthermore, well-founded and -tested EMT potentials are available [16]. For instance, the following Au properties have been well accounted for in the EMT: surface alloying [17], surface reconstructions [9], and bulk alloy diffusion [18]. Finally, gold is used in the VLS process to produce whiskers [19]. Needless to say, there are other experimentally motivated studies of, e.g., Si or Pt diffusion through liquid Au, but Au self-diffusion is here studied as a natural prerequisite.

Previous investigations [20] of liquid diffusivity utilizing a many-body potential (EAM) report that the local structure of the liquid transition metals Pt and Pd is quite insensitive to many-body interaction between atoms, at least near the solid-liquid transition. This is not very surprising since it is well known that the local structure is fairly insensitive even to rather different pair potentials due to the predominant influence of hard-core effects [1]. However, by going from a purely pairwise to a many-body potential, an increased diffusivity and a decrease in the efficiency of momentum transfer at short time scales is reported [20]. It seems therefore that going beyond pairwise potentials mainly affects the dynamics of a system. We will return to many-body effects in Sec. IV.

This paper shows that the structure, dynamics, and atomic diffusion in liquid gold can be realistically simulated. The quality of the interatomic potential is tested not only by its ability to reproduce the experimental liquid structure [5], but also through a comparison of calculated values of several thermal properties with existing experimental results. Obtained results are quite generally in very good agreement with experiment. One reason for this is the fact that the employed EMT description of the interactions between the Au atoms accounts for the main physical effects. In particular, the anharmonic part of the potential is well described in the EMT. This results in a good description of the thermal expansion coefficient and the melting transition [10,21].

Another reason is that the rapidity of liquid diffusion allows our molecular-dynamics simulation to follow the process over physically relevant time periods. This is often a problem for solids, where the diffusion is several orders of magnitude slower. In order to obtain good diffusivity statistics below the melting point, much larger systems and/or longer simulation times are required.

To the authors' knowledge, no investigations on the temperature dependence of the self-diffusion coefficient in liquid Au have been undertaken prior to this one, although results for the melting point diffusivity have been reported previously [22–24]. This is also an extensive high-accuracy diffusion study that covers the entire liquid temperature range of a nonsimple metal, employing a many-body potential.

The plan of the paper is the following. Section II gives a brief account of the EMT. The simulation method is described in Sec. III. In Sec. IV our results are presented and in Sec. V there is a discussion. Finally, Sec. VI provides our major conclusions.

II. EFFECTIVE-MEDIUM THEORY

Our capacity to calculate the total energy of a system of interacting atoms is limited, basically, by the size and the symmetry of the system. Increasing computer power, improvements in the field of numerical methods, and the presence of a working fundamental theory have together led to an enormous increase in the number of first-principles calculations that are available. Still, one is limited to systems or unit cells with up to about 50 atoms for such first-principles calculations. It is thus necessary to work with simpler models for larger systems. Such models may also produce physical insight.

The basic idea of the effective-medium theory is to cal-

culate the energy of an atom in an *arbitrary* environment by first calculating it in some properly chosen reference system, the effective medium, and then estimate the energy difference between the real system and the reference system [13]. For the latter an electron gas is chosen, so that the binding energy of the atom is easily obtained.

Based on the density-functional theory (DFT), the total energy of a system of interacting atoms is written as [13]

$$E_{\text{tot}} = \sum_i \left[E_c(i) + \Delta E_{\text{AS}}(i) + \Delta E_{1\text{el}}(i) \right], \qquad (1)$$

where the summation runs over all atoms in the system. Here the cohesive function $E_c(i)$ gives the energy of atom i in the reference system, while the atomic-sphere correction term ΔE_{AS} represents the energy associated with the overlap of atomic spheres, and the one-electron term $\Delta E_{1\text{el}}$ accounts for covalent effects beyond those present in the reference system. For free-electron-like and noble metals $\Delta E_{1\text{el}}$ is small and neglected here. ΔE_{AS} vanishes by definition for a system of close-packed atoms in a fcc structure at any lattice parameter, but is nonzero whenever the atomic configuration differs from the perfect fcc. The theory has been described in detail in Ref. [13]. The nine parameters for the potential employed in these simulations are taken from Ref. [16]. They are calculated *ab initio*, except for three parameters which are empirically fit to the 0 K bulk modulus, the cohesive energy, and the elastic constant C_{44}, respectively. We emphasize that the potential is derived for the solid, and not modified in any way to better account for liquid properties.

Results for the elastic properties in EMT have been reviewed in Ref. [9]. Instead of $C_{12} = C_{44}$, as given by pair potentials, EMT gives the relation $C_{11} = C_{12} + C_{44}$. For Au, the experimental values of the elastic constants give $(C_{12} + C_{44})/C_{11} = 1.06$, implying a mere 6% error in the EMT result. The EMT value for the ratio C_{12}/C_{44} is 3.6, as compared to the numbers 3.7 from experiments and 1 from pair-potential theory. For properties relevant for this study, such as surface relaxation [9], vacancy formation [10], melting temperatures, and entropy changes on melting [10], the EMT is doing reasonably well (for Au, see below).

III. SIMULATION DETAILS

Investigations of some static and dynamic properties of gold have been undertaken using two common simulation techniques. First, we have performed Monte Carlo (MC) simulations in the isobaric-isothermal, or constant-*NPT*, ensemble. The calculated densities have then been used as input for subsequent molecular-dynamics (MD) simulations in the microcanonical, or constant-*NVE*, ensemble. This means that in every MD simulation, regardless of temperature, the time-averaged pressure $\bar{P}$ of the system has been practically zero due to the relevant choice of density given by the MC simulations. Successful studies in this so-called constant-$NVE\bar{P}$ ensemble have been reported previously [23].

The two-stage process of first calculating the density and other thermal properties in one ensemble, and then utilizing the density to perform MD simulations in another ensemble, may seem somewhat tedious at first. The major reason for this choice of operational procedure is that there are reports

that constant-pressure MD simulations tend to overestimate self-diffusion coefficients due to large density fluctuations [23]. The self-diffusion coefficients reported in this study are thus calculated in an ensemble that does not allow for any density fluctuations in the MD simulation box, unlike the usual isobaric-isoenthalpic, or constant-*NPH*, and isobaric-isothermal ensembles.

The Monte Carlo simulations are performed in the full condensed-matter temperature range of Au (0–3080 K). A cubic slab of $5^3 = 125$ atoms situated in a perfect fcc structure is used as the starting point for all MC simulations. Periodic boundary conditions are imposed in all three directions. At each step of the simulation, two types of changes are introduced. They consist of displacing an atom from its geometric position, and changing the volume of the entire system using a breathing-box algorithm. The first change allows for atomic relaxations, while the other change is for maintaining the system at constant pressure. Whether or not a particular change is accepted is determined by using the algorithm of Metropolis *et al.* [25]. These steps are repeated a large number of times to achieve an equilibrium state. The acceptance ratios of the atomic displacements and volume changes are through a suitable choice of vibrational amplitudes held at approximately 50–60 % at each temperature. The system is initiated by making 1000 attempts at each degree of freedom (DOF), and data are then collected every 20 attempts per DOF up to a total of 6000 attempts per DOF. The potential energy and the instantaneous volume of the system (maintained at zero pressure) are extracted and a time average is made.

The molecular-dynamics simulations are performed in the liquid temperature range of 1450–3080 K. Cubic setups of $8^3 = 512$ and $10^3 = 1000$ atoms are used with periodic boundary conditions as in the MC case. At the start of the simulations, the atoms are placed at their perfect fcc lattice positions. The density is taken from the preceding MC calculations. Each setup is first initiated for at least 2000 time steps using the Andersen thermalization procedure [26] to reach the desired temperature through stochastic temperature control. When simulating at temperatures near the melting point, the perfect crystal is first heated to a high temperature to ensure total melting, and then gradually cooled down. The thermalization is then stopped and the system is allowed to evolve microcanonically for at least 20 000 time steps, saving every 20th configuration together with other relevant data. The equations of motion are numerically integrated using the velocity-Verlet algorithm [26] with a time step of $t = 2.70$ fs and $t = 2.16$ fs at temperatures below and above about 2300 K, respectively. The total-energy conservation of the algorithm during a microcanonical simulation improves with lower temperatures, the worst high-temperature case losing 0.5 meV per atom over 20 000 time steps.

Throughout all MC and MD simulations in this study, we have employed a potential that uses three (four) coordination shells in calculating the energy and four (five) shells in the neighbor list at temperatures below (above) 2300 K. The enlarged potential cutoff has been introduced to compensate for decreasing density at elevated temperatures. To minimize the risk of affecting the physics of the investigated system by this change, more than half a dozen simulations with the

larger cutoff have been performed at lower temperatures. No differences are detected in any of the investigated properties of Au.

In this study it is implicitly assumed that the electron gas remains in its ground state; this fact is invoked in the energy potential. However, this is not the case for higher temperatures. It is very hard to estimate how well high temperatures can be treated with a potential developed in and for the solid state. One way is to find a quantity that has been experimentally determined at high temperatures, and then notice when the simulation results start deviating markedly from these known values. The drawback of this method is that it will not necessarily reveal shortcomings in the potential. Another problem is the fact that it is usually very hard to find sufficiently accurate experimental values. We refer to Sec. IV for such an analysis. No signs whatsoever of physical shortcomings at higher temperatures have been detected.

The use of classical mechanics for the atoms (ions) is justified since the treated temperatures are far above the Debye temperature, $\theta_D = 165$ K for Au. The relevant effects of the degenerate Fermi gas of electrons are invoked in the effective-medium potential [13]. The treatment of atoms as classical particles instead of quantum-mechanical wave packets is also a very good approximation since the de Broglie wavelength of Au is less than 6 pm at all treated temperatures, far shorter than the interatomic distances.

One of the problems with all computer simulations on small systems consists of the inevitable fluctuations that occur in one or more of the thermodynamic quantities. In the microcanonical case the finite number of particles used in the simulations results in fluctuations in kinetic energy and pressure of the system. Since the temperature of the atomic system is directly connected to its kinetic energy, fluctuations in the latter quantity manifest themselves in hindering a precise specification of the temperature.

Another problem with using finite systems in computer simulations is that the imposed periodic boundary conditions easily can alter the physics of the actual systems. It is thus very important to examine the consequences that arise from using a small number of atoms. In order to get an estimate of size effects, simulations have been performed on larger systems. The simulation box has been enlarged from $5^3 = 125$ to $8^3 = 512$ atoms in the MC simulations and from $10^3 = 1000$ to $12^3 = 1728$ atoms in the MD calculations. The results from this investigation will be discussed in the next section.

IV. RESULTS

A. Monte Carlo results

The MC simulations provide several thermodynamic quantities describing the temperature-dependent behavior of the analyzed system. The potential energy and the atomic volume are extracted from each simulation and averages are made. Figure 1 shows the temperature dependence of the total energy per atom, $E_{tot} = E_{pot} + 3k_B T/2$. The atomic volume V at each temperature is converted into a lattice parameter, $a = (4V)^{1/3}$. This relation defines the ''lattice parameter'' also for the liquid phase. The lattice parameter is normalized to its calculated zero-temperature value $a_0 = 4.06$ Å, and the result is displayed in Fig. 2. The first-
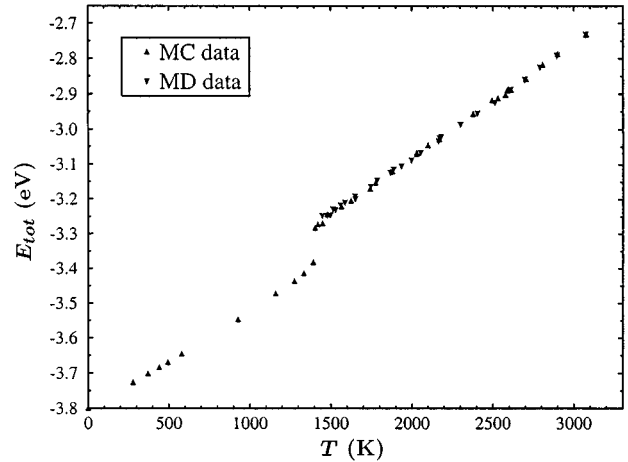

FIG. 1. The total energy per atom versus temperature.

order solid-liquid transition in energy and density gives a first indication of a relevant potential.

Thermal properties provide a useful check of the interatomic potential, since when atoms vibrate they sample wide portions of the functionals in the EMT potential, so that the behavior of the system depends on their form even relatively far from the 0 K fitting points. This is especially true for temperatures in the liquid regime.

As a test of the ability of the interatomic potential to account for low-temperature thermal properties, we have extracted the isobaric linear expansion coefficient $\alpha_l^s \equiv (\partial \ln a/\partial T)_P$ for the solid and found it to be 16.4×10^{-6} K^{-1}. This number is in good agreement with the experimental value [27] of 16.7×10^{-6} K^{-1}, indicating that the anharmonic terms in the potential seem very well described, at least for temperatures below the melting point. The experimental number and the result from the simulations are both obtained as averages over the temperature interval 293–1173 K.

To further test the potential, we have also extracted the isobaric heat capacity, $C_P \equiv (\partial H/\partial T)_P$, for the solid. The calculated $C_P^s = 28.5$ J/(mol K) is in good agreement with the
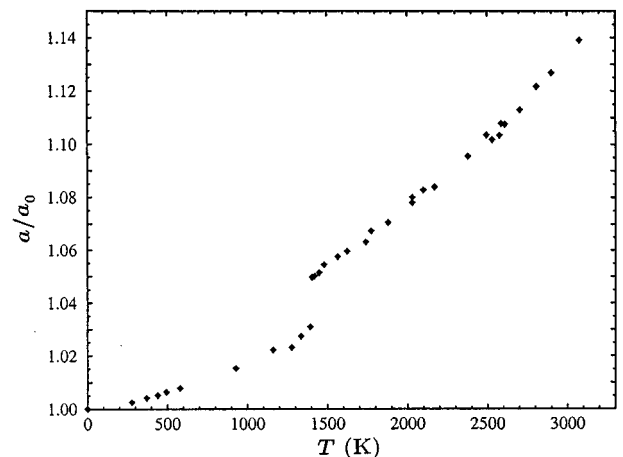

FIG. 2. MC results for the temperature dependence of the normalized lattice parameter, defined through the average atomic volume $a = (4V)^{1/3}$.
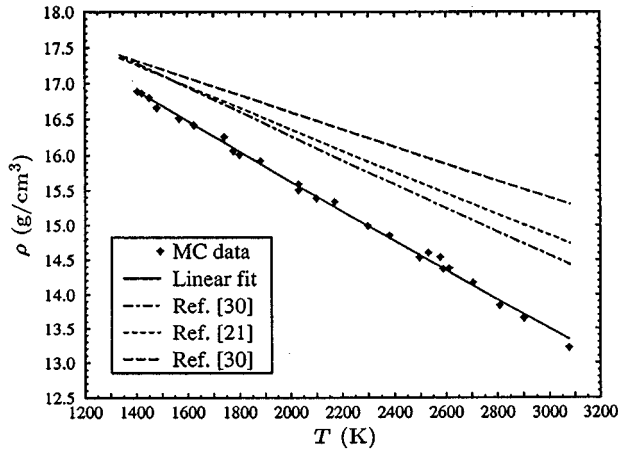
FIG. 3. The density of liquid Au as a function of temperature. Besides the linear fit, several experimental results are shown.
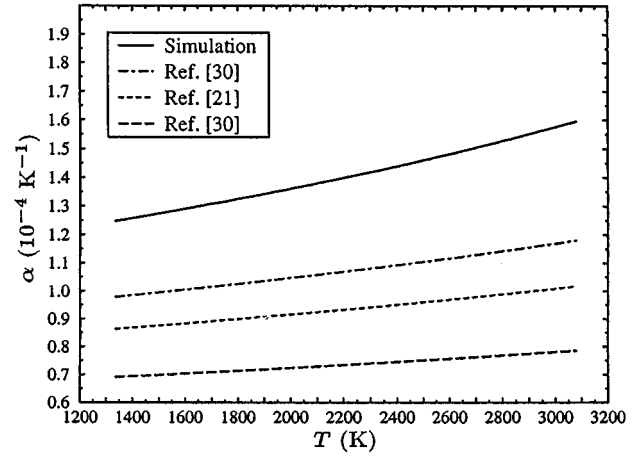

FIG. 4. The thermal expansion of liquid Au versus temperature, as calculated from a linearization of the liquid density according to Eq. (4). The other curves refer to experimental results.

corresponding experimental [28,29] value of 28.4 J/(mol K), once again verifying the accuracy of our many-body potential. These results are valid at temperatures in the approximate [30] range of 300–1300 K.

The solid-liquid transition temperature T^{s-l} is estimated to be 1398 K, slightly higher than the experimental value [31] for the melting temperature of 1337.58 K. The two values are relatively close, which is somewhat fortuitous since it is usually not possible to establish the exact melting temperature this way due to hysteresis effects. It is more appropriate to interpret the obtained solid-liquid transition temperature merely as a point of mechanical instability of an infinite single crystal. There are better ways of determining the melting temperature of an atomic system [32], but that is not the aim of this study.

The volume expansion upon melting ΔV^{s-l}, given by the magnitude of the discontinuity in Fig. 2, turns out to be 5.54%, in good agreement with the experimental value [6] of 5.5%.

The heat of melting per atom ΔH^{s-l}, appearing as a kink in the total energy at the melting point in Fig. 1, is extracted from the simulations and estimated to be 0.10 eV, a little low compared with the experimental values of 0.128 eV [27] and 0.132 eV [33,34].

A calculation of the isobaric heat capacity for the liquid results in $C_P^l = 30.91$ J/(mol K), which is in good agreement with the experimental value [28] of 31.19 J/(mol K). Besides this experimental result, valid at all liquid temperatures, another value of 29.29 J/(mol K), valid at temperatures 1338–1600 K, has been reported [27,34]. The striking linearity of the $E_{\text{tot}}(T)$ curve throughout the liquid range confirms the fact that the heat capacity is indeed, to a very good approximation, temperature independent in this state of matter.

Knowledge of the detailed temperature behavior of the liquid density is very important for, e.g., model calculations on inverse segregation [35]. A comparison between the calculated and experimental [27,36] liquid densities $\rho(T)$ is shown in Fig. 3. The rather large difference between experimental curves probably stems from the fact that the data are very old (1929, 1951). It is experimentally established that the density for many liquid metals is linear in temperature. This might in turn partly be a consequence of measurements

performed over limited temperature ranges. The linearity implies a temperature-independent density slope $\Lambda \equiv (\partial \rho / \partial T)_P$, and consequently a representation of the density in the form

$$\rho = \rho^{s-l} + \Lambda (T - T^{s-l}). \tag{2}$$

A linear fit [37] of Eq. (2) to our liquid density data, shown in Fig. 3, results in a value for the melting point density ρ^{s-l} of 16.9 g/cm^3, slightly low compared with the experimental [36] 17.4 g/cm^3. The same fit yields $\Lambda = 2.1$ mg/(cm^3 K), somewhat high compared with previously reported [27,36] values of 1.5, 1.2, and 1.7 mg/(cm^3 K). As seen in Fig. 3, our density values show a slight tendency towards curvature at higher temperatures, implying that Λ is not constant over the whole liquid range. This feature of Λ has been noticed for other metals as well, e.g., Al, Sn, and Ga [36]. We note, however, that the linear approximation for the temperature dependence of the liquid density is a very good one.

The isobaric volume expansion coefficient of the liquid, α_v^l, is related to the change of density with temperature, and is given by

$$\alpha_v^l \equiv \frac{1}{V} \left(\frac{\partial V}{\partial T} \right)_P = -\frac{\Lambda}{\rho}. \tag{3}$$

The number of simulations is not sufficient for a direct derivative to be calculated. Using the linear approximation given by Eq. (2), we can write down the temperature-dependent volume expansivity explicitly as

$$\alpha_v^l = \frac{-\Lambda}{\rho^{s-l} + \Lambda (T - T^{s-l})}. \tag{4}$$

We compare our results for this quantity with experimental findings in Fig. 4. The melting point expansivity turns out to be $\alpha_v^l(T^{s-l}) = 1.25 \times 10^{-4}$ K^{-1}, slightly higher than reported experimental [27,36] values of 0.86×10^{-4}, 0.69×10^{-4}, and 0.98×10^{-4} K^{-1}. A glance at the experimental isobaric thermal expansivities of the other two noble metals reveals that $\alpha_v^l(T^{s-l}) = 0.98 \times 10^{-4}$ K^{-1} and 1.0×10^{-4} K^{-1} for Ag and

TABLE I. Comparison between calculated and experimental thermal properties of Au.

	Simulation	Experiment	Unit
T^{s-l}	1398	1338[a]	K
ΔH^{s-l}	0.10	0.128,[b] 0.132[c,d]	eV/atom
C_P^s	28.5	28.4,[e] 28.4[f]	J/(mol K)
C_P^l	30.91	30.98,[e] 29.29[b,d]	J/(mol K)
ΔV^{s-l}	5.54	5.5[g]	%
ρ^{s-l}	16.9	17.4[h]	g/cm^3
Λ	2.1	1.5,[b] 1.2,[h] 1.7[h]	mg/(cm^3 K)
α_l^s	16.4	16.7[b]	10^{-6} K^{-1}
$\alpha_v^l(T^{s-l})$	1.25	0.86,[b] 0.69,[h] 0.98[h]	10^{-4} K^{-1}

[a]Reference [31].
[b]Reference [27].
[c]Reference [33].
[d]Reference [34].
[e]Reference [28].
[f]Reference [29].
[g]Reference [6].
[h]Reference [36].

Cu, respectively [6]. A summary of calculated and experimental thermal properties of Au is presented in Table I.

B. Molecular-dynamics results

The molecular-dynamics simulations provide information about both static and dynamic properties of the system under consideration. For each run, the kinetic and total energies are closely examined. The temperature is deduced from the momenta $\mathbf{p}_i$ of the atoms according to

$$\frac{3}{2}Nk_BT=\left\langle \sum_{i=1}^{N}\frac{1}{2m}\mathbf{p}_i^2 \right\rangle. \tag{5}$$

The total energy is extracted and checked for indications of possible energy-conservation violations, indicating the use of too large a time step. The results of the MC and MD total-energy calculations are plotted together in Fig. 1.

In order to verify that the simulation boxes indeed have a zero-pressure average, the instantaneous pressure of the system is calculated using the virial equation [26],

$$\mathcal{P}=\frac{N}{V}k_B\mathcal{T}+\frac{\mathcal{W}}{V}=\frac{1}{3V}\sum_{i=1}^{N}\frac{|\mathbf{p}_i^2|}{m}+\frac{1}{3V}\sum_{i=1}^{N}\mathbf{r}_i\cdot\mathbf{f}_i. \tag{6}$$

The thermodynamic pressure is obtained from a simple time average over the instantaneous pressure $\mathcal{P}$. Even though the limited size of the system results in quite large pressure fluctuations, reaching values of the order of 10^4 atm for the smallest slabs, the average pressure has remained zero within some 100 atm for all MD simulations reported in this study. A more exact value for the pressure requires an analysis of a larger number of configurations.

A good indicator of the structure of a given system of atoms is provided by the pair distribution function. This quantity is defined as

$$g(r)=\frac{V}{N^2}\left\langle \sum_{i}\sum_{j\neq i}\delta(\mathbf{r}-\mathbf{r}_{ij}) \right\rangle. \tag{7}$$
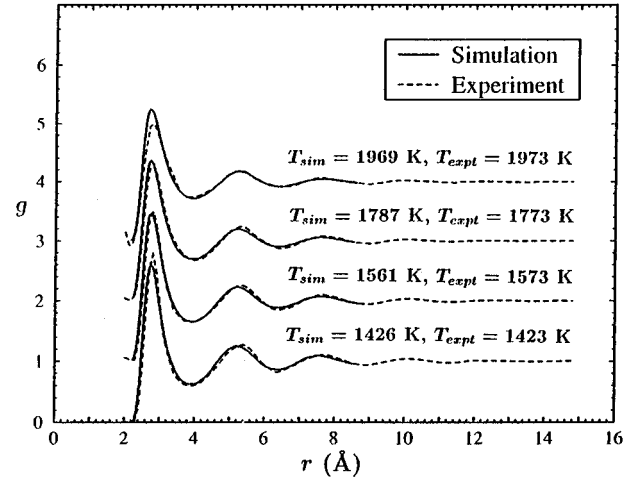

FIG. 5. The pair distribution function at various temperatures, calculated from MD simulations and compared with experimental findings. The g values correspond to the two lowest plots. The other pairs of calculated and experimental curves are shifted up by 1.0 relative to the previous pairs of plots.

Figure 5 compares the calculated normalized pair distribution function with experimental findings [5] at four temperatures in the liquid phase. The slight temperature difference between compared pair distribution functions is a consequence of simulating in the microcanonical ensemble, where the thermalization procedure and fluctuations in the kinetic energy can prevent the exact setup temperature from being reached in simulations. Within these small temperature differences, the overall agreement is very good, however, lending some support to the ability of the interatomic EMT potential to account for intermediate-temperature properties of liquid Au. The quantitative accuracy of the experimental curve at 1973 K is reported to be inferior to the other measurements [5], which may explain why the main peak is somewhat higher than in our calculation. The very small differences between the compared near-melting-point pair distribution functions are not as easily explained, but they are not a consequence of incomplete melting in the simulation.

The self-diffusion coefficient D_s is calculated from the slope of the mean-square displacement curve $f(t)$ of the atoms according to the Einstein equation

$$6D_st=\langle[\Delta\mathbf{R}(t)]^2\rangle\equiv f(t), \tag{8}$$

where

$$f(t)=\frac{1}{N_a}\frac{1}{N_f/2}\sum_{i=1}^{N_f/2}\sum_{j=1}^{N_a}\sum_{k=0}^{N_f/2}[\mathbf{R}(i_j+k_j)-\mathbf{R}(i_j)]^2. \tag{9}$$

In these equations, N_f is the number of configurations that are examined and N_a is the number of atoms in the system. The last equation illustrates how we have taken advantage of a dynamic origin to improve on our statistics. This way of calculating $f(t)$ produces points on the mean-square displacement curve with constant statistics [38]. For example, if $N_f=1000$, each of the 500 points on the $f(t)$ curve for a 1000-atom slab will be an average of 500 000 values.
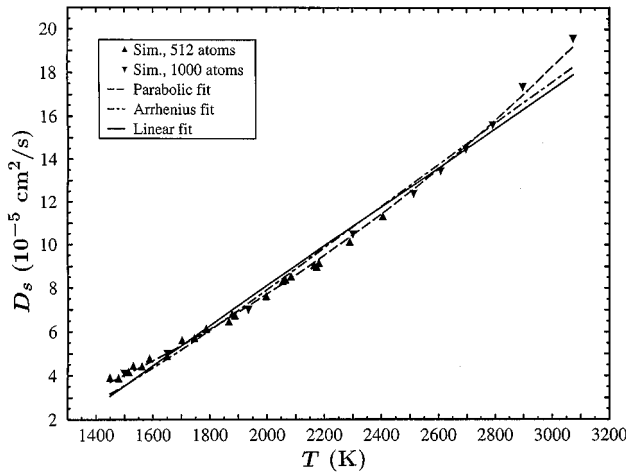
FIG. 6. The diffusivity of liquid Au as a function of temperature. The estimated uncertainties in temperature and diffusivity are too small to be drawn in the figure (see Sec. IV). The data can also be found in Table II.

TABLE II. Self-diffusion coefficients of liquid Au calculated from MD simulations. For error estimates, see Sec. IV.

T (K)	D_s (10^{-5} cm^2/s)
1449	3.90
1479	3.87
1500	4.12
1514	4.18
1531	4.43
1561	4.41
1588	4.77
1650	4.90
1651	5.02
1702	5.60
1746	5.70
1787	6.11
1787	6.13
1866	6.50
1878	6.85
1879	6.80
1935	7.03
1998	7.61
2055	8.30
2064	8.36
2084	8.51
2165	9.03
2173	8.97
2182	9.14
2290	10.11
2301	10.50
2405	11.32
2513	12.42
2608	13.48
2697	14.49
2792	15.61
2897	17.37
3073	19.59

The choice of time interval between investigated consecutive configurations in this study optimizes the ratio between amount of statistically uncorrelated data and required simulation time. The number of values that is averaged over in Eq. (9) scales linearly with the number of atoms in the system and quadratically with the number of examined configurations. In calculating diffusivities with this algorithm, it is therefore more time efficient to use a smaller slab, if possible, and simulate for longer times.

The results of our diffusion investigations are illustrated in Fig. 6 and also tabulated in Table II. Previously reported ''near-melting-point'' diffusivities of 3.75×10^{-5} cm^2/s, obtained from computer simulations [23], 2.75×10^{-5} cm^2/s, calculated utilizing viscosity measurements [24], and 2.1×10^{-5} cm^2/s, an experimental value [22], are not included in the figure. One reason for this is that, in all three cases, a value for the temperature is not stated. Another reason, concerning the last value, is that we have not been able to verify the claimed diffusivity from an examination of the original reference.

The fluctuations in kinetic energy during the MD simulations bring about an estimated uncertainty of 0.08% in reported temperatures, which at most means a temperature spread of 2.5 K near the boiling point. Thanks to the efficient algorithm for calculating diffusivities, and the large number of uncorrelated configurations, the estimated uncertainty in the self-diffusion coefficients is at most 0.3% for the 512-atom slab and less than 0.1% for the 1000-atom slab. The error bars of these two quantities are too small to be drawn in Fig. 6. For errors arising from the use of a finite-size system, see below.

Our main goal with this work is to present a collection of diffusivity data for liquid Au. This information can be used for comparisons with theoretical predictions of various diffusion models. The large abundance of these models, and the lack of certain thermal data, allow us at this stage only to make very selective comparisons. More detailed studies of selected diffusion models are in progress [39]. We will here focus on the qualitative temperature dependence of the diffusion coefficient, make a few comparisons with common

analytical expressions, and whenever appropriate refer to diffusion theories that predict such a behavior. A discussion on physical aspects of diffusion models in general is presented in the next section.

The first fit we examine has a temperature dependence given by the empirical Arrhenius functional form,

$$D_s = D_0 \exp^{-Q/k_B T}, \qquad (10)$$

which when fitted to our diffusivity data, yields an activation energy $Q = 0.41$ eV and a prefactor $D_0 = 8.69 \times 10^{-4}$ cm^2/s. Although none of the existing diffusion models we have encountered predicts this temperature dependence of the diffusivity, the above form is widely used to present diffusion measurements. The second fit is linear in temperature, as foretold to first order by several diffusion models [40,41]. The results of these fits are displayed in Fig. 6. Two facts are immediately apparent. First, it is seen how very hard it can be to distinguish between the linear and Arrhenius forms, even over a wide temperature range. Second, it is evident

that neither of the two forms accounts very well for the calculated diffusion behavior at low and very high temperatures.

The third fit is quadratic in temperature, as proposed by several theories [42,43], and certainly looks the best of the three candidates. The χ^2 ratios between the parabolic, Arrhenius and linear relations are 1:9:12. It is seen in Fig. 6 how the parabolic curve very neatly picks up not only the extreme low- and high-temperature points, but also the intermediate-region points. A two-parameter power fit, $D_s = kT^\delta$ (not shown in the figure), returns $\delta = 2.08$ as the most favorable power for the temperature dependence of the diffusivity.

It is very interesting to note that recent high-accuracy self-diffusion measurements in microgravity present the same T^2 dependence for liquid Pb, Sb, and In [44]. These measurements back up previous results from an earlier space mission, where also liquid Sn was found to obey the T^2 law [45]. The estimated error in diffusivity is as low as about or below 1.5% and 1.0% for the two missions, respectively, mainly due to the absence of any convectional interferences. Moreover, a two-parameter power fit to the measured $D_s(T)$ dependence for liquid Pb returned [44] $\delta_{Pb} = 2.05 \pm 0.05$, in excellent agreement with our $\delta_{Au} = 2.08$. It is also noteworthy that D_s values from space experiments are about 20–40 % lower than the best ground based values, a clear indication of convection contributions in ground experiments [45].

These microgravity experiments are all performed on nonsimple metals and are undoubtedly among the most accurate diffusivity measurements performed to this date. The agreement between these experiments and our simulations is therefore yet another indication that the EMT description works well in describing liquid dynamics.

As already pointed out in Sec. I, the diffusivity seems to increase by invoking many-body contributions to the interatomic potential in computer simulations. We are at this point compelled to believe that one reason for this is that the many-body potential allows for a more well-described thermal expansion than common pair potentials do. Naturally, further investigations in the spirit of the one by Chen *et al.* [20] is needed to clarify this issue [39].

Most computer simulations of liquids utilize an *effective* pair potential that is optimized by some kind of fitting procedures in order to describe a system well at, e.g., a certain temperature and density. This is an implicit way of invoking many-body effects. In order to look at the same system in another thermodynamic ambient, a new effective potential must be derived. Such potentials can thus not be very reliably used to assess, e.g., the temperature dependence of the self-diffusion coefficient. It is more appropriate for this purpose to maintain the same potential throughout the variation of the intensive variables, as done in this study. This, however, does not work very well for pair potentials. One major reason for this is that the many-body contributions no longer can be accounted for. Pair potentials of this kind tend to underestimate the thermal expansion, resulting in a system of too high a density. This is analogous to applying an external hydrostatic pressure to the real system, a condition that is well known for effectively decreasing the diffusion coefficient.
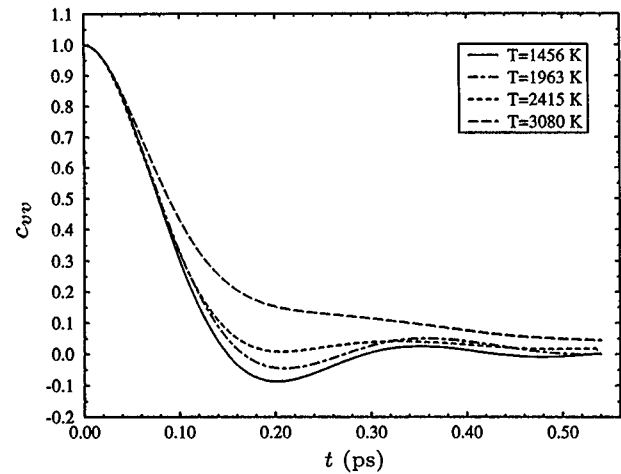

FIG. 7. The normalized velocity correlation function at various temperatures in the liquid phase of gold.

A first indication of the dynamics in a system is obtained by examining the velocity correlation function (VCF). This function relates the velocity of an atom i at a certain time $\tau = 0$ to its velocity at a later time, $c_{vv} = \langle \mathbf{v}_i(t) \cdot \mathbf{v}_i(0) \rangle / \langle \mathbf{v}_i(0) \cdot \mathbf{v}_i(0) \rangle$. It is one of the simplest, yet most important examples of time correlation functions. For instance, when integrated in time, it produces the diffusion constant. The procedure for extracting this quantity is analogous to the one for calculating diffusivities. The results at some selected temperatures are displayed in Fig. 7, and commented on in Sec. V, in connection with a discussion of atomic dynamics.

It is at this point appropriate to discuss the size effects that arise from using finite simulation cells. They are surprisingly small. It is actually quite remarkable that the small simulation box of 125 atoms used in the Monte Carlo simulations qualitatively and quantitatively produces very good results. Several MC simulations on slabs of 216 and 512 atoms with periodic boundary conditions imposed in all three directions show (within the estimated margins of error) no deviations from the results of the smaller slab as concerns atomic volume and potential energy. Only the fluctuations in these quantities are slightly decreased.

The molecular-dynamics simulations seem also to be remarkably insensitive to the system size. The differences in diffusivity that emerge from the few MD runs performed on larger slabs of 1728 atoms all fall within 1% of the smaller systems. Again, the small number of simulations on the larger simulation box prevents a detection of possible trends. If anything, it is believed that larger systems would slightly increase the self-diffusion coefficients, rather than the opposite. Similar size insensitivities (of static properties) have been reported previously [46].

V. DISCUSSION

The few scattered diffusivity data that presently exist for pure metallic liquids suffer from large uncertainties. The only exception to this fact is due to recent high-accuracy data provided by means of micro gravity measurements. Unfortunately, such experiments are by their nature very scarce. Judging from the development of this field over the last ten years or so, it seems likely that the ever growing use of

computer simulations eventually will change this situation, through the buildup of an extensive database of high-accuracy diffusivity data that can be cross-checked with, e.g., microgravity results. It is the intention of this study to provide a small contribution to such a collection of diffusion coefficients.

After the explosion of diffusion models in the 1970s, almost a total stagnation has occurred. Apart from a variety of hard-sphere models [47–49], there is an abundance of atomic transport theories such as the hole theory [50], the free volume theory [51,52], the significant structure theory [40], the quasicrystalline theory [53], the linear trajectory theory [41], and the fluctuation theory [42,54]. Comprehensive reviews of many other diffusion models have been written previously [6,55,56].

Not very surprisingly, the majority of the existing models are influenced by either solid or gas theories, as indicated by their names. However, the symmetries present in ideal solids and gases allow detailed characterizations of states, and thus accurate descriptions. The disorder of liquids gives room only for models that are harder to verify. Most of the model theories predict a complicated temperature dependence of the diffusivity. Some utilize concepts like viscosity [40], surface tension [57], or compressibility [54]. Hereby they may be even harder to verify, as the problems of measuring these quantities are much the same as in diffusion measurements.

With the currently available precision, the temperature range accessible for liquids is on the verge of being too narrow for a distinction to be made between different temperature dependencies of the diffusion coefficient. As indicated in Sec. IV, and reported previously [58], it is very easy to fit several totally different functional forms to one set of data even over the full liquid range. For now, however, diffusion models have to be viewed from their level of physical understanding.

Just by glancing at a computer screen during a simulation (with a reasonable description of the atomic interaction), one can get an impression of what is physically sound. A feature that immediately catches one's attention is that self-diffusion in liquids certainly looks like a highly collective process, in which many atoms make small correlated moves. Detailed trajectory studies, where we have tagged and closely followed the motion of individual atoms, directly verify this view of diffusion. An illustration of a typically observed diffusion behavior is shown in Fig. 8. This kind of microdynamical behavior was suspected already in the 1970s [56], and seems, at present, to be commonly accepted. There are, no doubt, more advanced ways of examining the detailed dynamics of atoms in metallic liquids, e.g., by examining the Van Hove distribution function [4]. However, the mentioned crude technique is presently adequate for our purposes.

Details of the dynamic behavior of diffusing atoms can also be detected in the VCF shown in Fig. 7. The first minimum is markedly more shallow than in the solid case, indicating a heavily reduced caging effect. This is a clear implication of the increased mobility atoms in a liquid have compared with atoms in a solid. With increased temperatures, this initially negative-valued minimum becomes even more shallow, and is eventually smeared out.

One direct result of these observations is that the diffusion model most consistent with our results and the thus provided
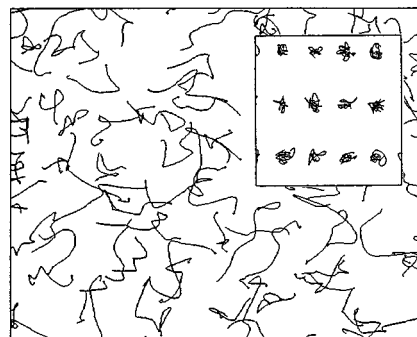

FIG. 8. A two-dimensional projection of a typical trajectory plot of the atomic motion in a metallic liquid. The atoms are tagged and followed for 1.3 ps. Inserted in the figure is a corresponding plot for a solid (both boxes have the same area, even if the scales are different).

view of the physics of liquids is the fluctuation model of Swalin [42,54]. This theory of diffusion depends on local density fluctuations, but unlike many other models [43,50–52] that depend on unphysical assumptions about discrete jumps over interatomic distances, it does not require the creation of a critical void volume. So far, one can only notice that it has met certain success, and has been regarded as a "remarkably good" [56,59] model. The first version [42] of the fluctuation model predicts a T^2 dependence of the self-diffusivity, while the second, revised, version [54] proposes a $T\beta_T$ dependence under isobaric conditions. At present, the lack of compressibility data prevents a direct test of this prediction. Calculating the isothermal compressibility from MC simulations requires larger systems than we employ in this study. Utilizing the experimentally available adiabatic compressibility as a first approximation yields a good qualitative agreement over the narrow temperature range set by the experiment [39].

Another consequence of our observations concerns the question of activation energies. As previously pointed out by Nachtrieb [59], the use of an Arrhenius expression for representing the temperature dependence of the diffusivity in liquids has, basically, only historical reasons. The concept of an activation energy has simply been adopted from solid-state vacancy or impurity diffusion upon findings that diffusion rates in the liquid conveniently can be fitted to an exponential dependence on $1/T$. At the time, diffusion in liquids was thought to take place via a vacancy mechanism, in the same manner as in solids, thereby somewhat justifying this formalism. Today, we know better. We also know that an Arrhenius temperature behavior of the diffusion coefficient is more an exception than a rule [59–62]. Still, this form of representation is readily utilized, and seems to be "the accepted law in most of the literature" [44], in spite of its early abandonment by mainly liquid theorists and the issued warnings [56,59,63]. The existing diffusion data, which encompass around a dozen liquid metals [6,56], are with few exceptions presented in the Arrhenius formalism. The situation is the same for results from computer experiments such as this one [23,64]. We believe this use of the Arrhenius formula in liquid metals should have been abandoned long ago. We will now try to present some aspects of the atomic dynamics of liquid metals.
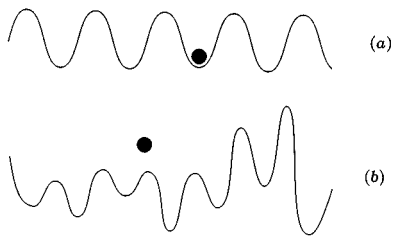
FIG. 9. Atoms in a stylized one-dimensional potential energy slice of a solid and a liquid. In the solid (a) this picture is static, whereas in the liquid (b) it changes continuously.

In the solid, an atom has a relatively low kinetic energy to surpass the ridges of time-independent energy barriers (adiabatic approximation applicable) it is surrounded with. It will therefore vibrate in a local energy minimum until it, after many vibrations, eventually makes a jump over one of the lower barriers into a new position. In this state of matter, the barriers accessible to diffusing atoms are few and of well-defined sizes. Usually there is one specific route, a diffusion channel, with the lowest-energy barrier to motion that the atoms will tend to take. The magnitude of this barrier can, for instance, be extracted from fitting experimental findings of diffusivity to Eq. (10). Figure 9(a) illustrates this view of the diffusion process in solids.

Extending this picture to the liquid region is anything but trivial. Unlike in the solid, there is no static background to give rise to well-defined energy barriers in the liquid. There is instead a constant motion of *all* of the constituent atoms. The vibrations in the solid are thus essentially the motion in the liquid. The rapid atomic motion in liquids, taking place on the femtosecond time scale, makes it impossible to introduce order in the sense of viewing diffusion as jumps over a certain energy barrier. There will at all times exist a broad spectrum of close-lying energy barriers [65]. Recently, progress has been made using the liquid-state normal mode analysis [65,66]. The dynamics of a liquid in a certain configuration is in this theory described by oscillations obtained from the stable normal modes and saddle points obtained from the unstable normal modes.

Naturally, it is in principle possible to view the diffusion processes in a liquid as hops over a certain *effective* energy barrier. This is the core of the Arrhenius formalism. The price to pay for maintaining this solid-state picture of diffusion is that an entire set of energy barriers has to be considered and that the activation energy will be temperature dependent, as foretold by Swalin [42,54]. Since the kinetic energy in the liquid region is of roughly the same size as the potential energy, the energy situation of Fig. 9(a) will change markedly, as schematically depicted in Fig. 9(b). Now, at a specific temperature, a diffusing atom will effortlessly sail over the lower barriers and there will, on average, exist a certain effective energy barrier that will give rise to an activation energy that is measurable through experiments. If the temperature is changed, the atom will face another effective energy barrier and thus the activation energy will be temperature dependent.

This picture implies an effective activation energy that increases monotonically with temperature, even though, at this point, it is hard to make any statements about the exact nature of this temperature dependence of the activation energy. It is directly related to the detailed energy barrier distribution in the liquid and may very well be system dependent. It is therefore very misleading to talk about a single activation energy in liquid metals. Obviously, others have run into a similar nomenclature dilemma, thereby the appearance in literature of the so-called ''apparent'' activation energy [6,54,59]. In addition, it has been argued recently that the precise distribution of energy barriers plays a crucial role in determining the temperature dependence of the self-diffusion coefficient [65].

Since the temperature dependence is far from established, we advocate tabular-form presentations of diffusivity data in the future. The usage of parallell computers now enables extensive simulations on very large systems that provide high accuracy. Together with improving experimental techniques, this should soon allow for an accurate assessment of the temperature dependence of the self-diffusion coefficient, and an answer to the question of how general such a behavior is for different atomic systems.

VI. CONCLUSIONS

In conclusion, we have shown that the EMT many-body potential for solid Au very accurately accounts for structural, thermal, and dynamical properties of the liquid phase of this metal. The combination of MC simulations within the isobaric-isothermal ensemble and MD simulations in the microcanonical ensemble is found to work very well, even at high temperatures. For the first time, extensive high-accuracy diffusivity data resulting from calculations with a many-body potential are presented for a metal, covering the entire liquid temperature range. This is also the first study concerning the diffusivity of the technologically very important metal Au that goes beyond the melting point. A T^2 law is calculated, in concurrence with very recent microgravity measurements on other nonsimple metals. A discussion on some microscopic aspects of the dynamics of atoms in metallic liquids is presented. The use of an Arrhenius expression to represent diffusivity data in metallic liquids is reexamined and, again, found to be inadequate and misleading.

ACKNOWLEDGMENTS

[1] J. P. Hansen and I. R. McDonald, *Theory of Simple Liquids*, 2nd ed. (Academic Press Inc., London, 1986).

[2] H. L. Friedman, *A Course in Statistical Mechanics* (Prentice-Hall, Englewood Cliffs, NJ, 1985).

[3] J. P. Boon and S. Yip, *Molecular Hydrodynamics* (Dover, New York, 1991).

[4] P. A. Egelstaff, *An Introduction to the Liquid State*, 2nd ed. (Oxford University Press, Oxford, 1992).

[5] Y. Waseda, *The Structure of Non-crystalline Materials* (McGraw-Hill, New York, 1980).

[6] T. Iida and R. I. L. Guthrie, *The Physical Properties of Liquid Metals* (Oxford University Press, Oxford, 1988).

[7] J. D. Weeks, D. Chandler, and H. C. Andersen, J. Chem. Phys. **54**, 5237 (1971).

[8] M. S. Daw, S. M. Foiles, and M. I. Baskes, Mater. Sci. Rep. **9**, 251 (1988).

[9] K. W. Jacobsen, Comments Condens. Matter Phys. **14**, 129 (1988).

[10] F. Ercolessi, M. Parrinello, and E. Tosatti, Philos. Mag. A **58**, 213 (1988).

[11] M. S. Daw and M. I. Baskes, Phys. Rev. Lett. **50**, 1285 (1983).

[12] F. Ercolessi, E. Tosatti, and M. Parrinello, Phys. Rev. Lett. **57**, 719 (1986).

[13] K. W. Jacobsen, J. K. Nørskov, and M. J. Puska, Phys. Rev. B **35**, 7423 (1987).

[14] P. Stoltze, J. K. Nørskov, and U. Landman, Phys. Rev. Lett. **61**, 440 (1988).

[15] L. B. Hansen, K. Stokbro, B. I. Lundqvist, K. W. Jacobsen, and D. M. Deaven, Phys. Rev. Lett. **75**, 4444 (1995).

[16] P. Stoltze, *Simulation Methods in Atomic-Scale Materials Physics* (Polyteknisk Forlag, Lyngby, 1997).

[17] L. P. Nielsen, F. Besenbacher, I. Stensgaard, E. Lægsgaard, C. Engdahl, P. Stoltze, K. W. Jacobsen, and J. K. Nørskov, Phys. Rev. Lett. **71**, 754 (1993).

[18] A. Bogicevic, Diploma thesis, Chalmers University of Technology and Göteborg University, Applied-Physics Report No. 95-17, 1995.

[19] R. S. Wagner, in *Whisker Technology*, edited by A. P. Levitt (Wiley-Interscience, New York, 1970).

[20] K. Chen, Q. Li, and X. Chen, Acta Phys. Sin. **42**, 283 (1993).

[21] H. Häkkinen and M. Manninen, J. Phys. Condens. Matter **1**, 9765 (1989).

[22] O. K. Belousov, Izv. Akad. Nauk. SSSR Met. **4**, 37 (1994).

[23] J. Mei and J. W. Davenport, Phys. Rev. B **42**, 9682 (1990).

[24] J. W. Nowok, Scr. Metall. Mater. **29**, 931 (1993).

[25] N. Metropolis, A. W. Rosenbluth, M. N. Rosenbluth, A. H. Teller, and E. Teller, J. Chem. Phys. **21**, 1087 (1953).

[26] M. P. Allen and D. J. Tildesley, *Computer Simulation of Liquids* (Oxford University Press, Oxford, 1987).

[27] E. A. Brandes, *Metals Reference Book*, 6th ed. (Butterworths, London, 1983).

[28] R. Hultgren, P. D. Desai, D. T. Hawkins, M. Gleisner, K. K. Kelley, and D. D. Wagman, *Selected Values of the Thermodynamic Properties of Elements* (American Society for Metals, Metals Park, OH, 1973).

[29] Y. S. Touloukian and E. H. Buyco, *Thermophysical Properties of Matter* (IFI/Plenum, New York, 1970), Vol. 4.

[30] These three values (one simulated plus two experimental) are averages of the heat capacity in the temperature intervals of 278–1336, 298–1336, and 400–1164 K, respectively.

[31] J. Emsley, *The Elements*, 3rd ed. (Oxford University Press, Oxford, 1996).

[32] J. R. Morris, C. Z. Wang, K. M. Ho, and C. T. Chan, Phys. Rev. B **49**, 3109 (1994).

[33] W. Lange, Z. Metallkd. **57**, 653 (1966).

[34] O. Kubaschewski and C. B. Alcock, *Metallurgical Thermochemistry*, 2nd ed. (Pergamon Press, Oxford, 1979).

[35] S. Chang and D. M. Stefanescu, Acta Mater. **44**, 2227 (1996).

[36] D. J. Steinberg, Metall. Trans. **5**, 1341 (1974).

[37] All fits to data in this study are performed by means of the least-squares method.

[38] An alternative way is to replace $N_f/2$ in the first sum with N_f and $N_f/2$ in the second sum with $(N_f - i_j)$. This choice will produce points with statistics linearly decreasing to zero from twice as good statistics as in the chosen method.

[39] L. B. Hansen and A. Bogicevic (unpublished).

[40] S. M. Breitling and H. Eyring, in *Liquid Metals: Chemistry and Physics*, edited by S. Z. Beer (Marcel Dekker, New York, 1972).

[41] S. A. Rice and N. H. Nachtrieb, Adv. Phys. **16**, 351 (1967).

[42] R. A. Swalin, Acta Metall. **7**, 736 (1959).

[43] A. Lodding, Z. Naturforsch. Teil A **27**, 873 (1972).

[44] G. Frohberg, K. H. Kraatz, A. Griesche, and H. Wever, in *Proceedings of the Norderney Symposium on Scientific Results of the German Spacelab Misson D-2: Norderney, Germany, 1994* (Wissenschaftliche Projektführung D-2, RWTH Aachen, 1995).

[45] Y. Malmejac and G. Frohberg, in *Fluid Sciences and Materials Science in Space, A European Perspective*, edited by H. U. Walter (Springer-Verlag, Berlin, 1987).

[46] J. M. Holender, J. Phys. Condens. Matter **2**, 1291 (1990).

[47] P. Ascarelli and A. Paskin, Phys. Rev. **165**, 222 (1968).

[48] C. J. Vadovic and C. P. Colver, Philos. Mag. **21**, 971 (1970).

[49] P. Protopapas, H. C. Andersen, and N. A. D. Parlee, J. Chem. Phys. **59**, 15 (1973).

[50] J. Frenkel, *Kinetic Theory of Liquids* (Oxford University Press, London, 1946).

[51] M. H. Cohen and D. S. Turnbull, J. Chem. Phys. **31**, 1164 (1959).

[52] D. S. Turnbull and M. H. Cohen, J. Chem. Phys. **52**, 3038 (1969).

[53] G. Careri and A. Paoletti, Nuovo Cimento **2**, 574 (1955).

[54] R. A. Swalin, Z. Naturforsch. Teil A **23**, 805 (1968).

[55] J. B. Edwards, E. E. Hucke, and J. J. Martin, Met. Rev. **120**, 13 (1968).

[56] N. H. Nachtrieb, Ber. Bunsenges. Phys. Chem. **80**, 678 (1976).

[57] J. W. Nowok, Acta Metall. Mater. **42**, 4025 (1994).

[58] N. H. Nachtrieb, in *Proceedings of the International Conference on the Properties of Liquid Metals, Brookhaven, 1966*, edited by P. D. Adams, H. A. Davies, and S. G. Epstein (Taylor & Francis, London, 1966).

[59] N. H. Nachtrieb, in *Proceedings of the Second International Conference on the Properties of Liquid Metals, Tokyo, 1972*, edited by S. Takeuchi (Taylor & Francis, London, 1972).

[60] S. J. A. Larsson, Licentiate thesis, Chalmers University of Technology and Göteborg University, 1974.

[61] M. Shimoji, *Liquid Metals* (Academic Press, London, 1977).

[62] M. Shimoji and T. Itami, *Atomic Transport in Liquid Metals* (Trans Tech Publications, Aedermannsdorf, 1986).

[63] T. E. Faber, *An Introduction to the Theory of Liquid Metals* (Cambridge University Press, Cambridge, England, 1972).

[64] J. M. Holender, Phys. Rev. B **41**, 8054 (1990).

[65] T. Keyes, J. Chem. Phys. **101**, 5081 (1994).

[66] G. Seeley and T. Keyes, J. Chem. Phys. **91**, 5581 (1989).